Formation of Gas Bubbles at Submerged Orifices

W. B. HAYES, III, B. W. HARDY, and C. D. HOLLAND

Agricultural and Mechanical College of Texas, College Station, Texas

The formation of air bubbles at constant pressure at submerged orifices was investigated for several liquids. The frequency of formation of the bubbles was determined by the use of a stroboscope, and the rate of gas flow was measured with conventional rotameters. Several orifices having diameters ranging from 0.0794 to 0.397 cm. were employed, and the gas flow rate was varied from about 0.1 cc. (at standard conditions)/sec. to about 150 cc./sec. It was found that the formation of bubbles could be correlated with the physical variables of the system by the application of Newton's second law of motion to the bubble at the instant just prior to its release from the orifice.

Gas, as a dispersed phase, plays a significant role in numerous physical and chemical processes. This is reflected by the attention given in the literature to the formation of gas bubbles at capillary tubes, orifices, and other devices submerged beneath liquid surfaces (*1, 2, 4, 5, 6*). In the experiments described herein the bubbles were formed at approximately constant pressure within the gas chamber (Figure 1) by passing air through orifices each of which was submerged in several liquids in turn. Correlation of the physical variables involved was achieved through the application of Newton's second law of motion.

It has been established that at very low rates of air flow the size of the bubble is nearly independent of the flow rate and is determined primarily by the orifice diameter, the surface tension, and the liquid density. At higher or intermediate rates of gas flow the size of the bubble becomes dependent upon the rate of gas flow through the orifice, as shown by Davidson *et al.* (*1*). At very high rates of gas flow Leibson *et al.* (*6*) demonstrated that the apparent jet of air issuing from the orifice is actually a series of closely spaced, irregular bubbles which undergo further separation upon rising through the liquid.

The influence of the volume of the gas chamber (Figure 2) and other physical dimensions of the apparatus on the formation of bubbles has been pointed out by Hughes *et al.* (*4*), who also observed that the effect of the chamber volume was not considered in the treatment of many of the data in the literature. Davidson *et al.* (*1*) demonstrated that as long as the volume of the gas chamber was less than a critical size it did not affect the formation of bubbles. For a given orifice diameter and gas flow rate the volume of the bubbles formed increased as the chamber volume was increased until approximately constant pressure within the gas chamber was approached. Most of the experiments reported in the literature were carried out with both capillary tubes and relatively small gas-chamber volumes; however in some instances Davidson (*1*) and Leibson (*6*) did use chamber volumes large enough to insure the formation at constant pressure within the gas chamber.

Since the majority of the bubble type of contactors employed in industrial applications operate at constant gas-chamber pressure and since such data are scarce, this investigation was undertaken.

EXPERIMENTAL

Experimental Apparatus

The equipment employed to collect the data used in the correlations consisted of the following major items: a column 10 in. in diameter and 72 in. long, an orifice holder 2 in. in diameter and 22 in. long, three rotameters, a Strobotac and Strobolux attachment, two manometers 60 in. long, six orifice plates, a wet-test gas meter, and two pressure regulators.

Figure 3 is a schematic flow diagram of the equipment. The pressure of the air entering the column through the orifice holder, located at the bottom of the column, was measured with respect to atmospheric pressure with a 60-in. manometer in which water was used as the fluid. Gas temperatures were measured with dial thermometers, and a mercury-filled glass thermometer was used to measure the temperature of the liquid, which could be read to within 0.1°C. The orifice plates employed to obtain the data used in the correlations shown herein were made of stainless steel plate 0.318 cm. thick. The diameters of the orifices were 0.0794, 0.159, 0.238, 0.318, 0.397, and 0.635 cm. The orifice holder, shown in Figure 1, was constructed from a section of stainless steel tubing. The rotameters used to measure the rates of gas flow were calibrated by with a wet-test meter.

Physical Properties of the Liquids

The interfacial tensions of the liquids with respect to air were measured with a Du Nouy direct-reading tensiometer, the viscosities were determined with a Stormer viscosimeter, and densities of the liquids were measured with a Westphal balance. The experimental values so obtained were in good agreement with those in the literature. These results are given in reference *3* and are also on file.* The correlations, Equations (27) and (28), were based on the results of 504 experiments. In all of them either pure liquids or mixtures of pure liquids which wet the orifice were employed, and the chamber volume was held constant at 1,322 cc. A wide variation in the viscosity of the liquid phase was obtained by the use of aqueous solutions of glycerine. Other liquids employed in this series of experiments were kerosene and isopropyl alcohol. In seventy-three other experiments the viscosity of the liquid phase was altered by the use of silicone additives. A chamber volume of 1,322 cc. was also employed in these runs. The effect of the geometry of the chamber volume on the formation of bubbles was investigated in a series of forty-one experiments. Throughout the entire investigation air was used as the gas phase.

Operation of Equipment

Prior to the initiation of a series of experiments the orifice holder was placed under pressure to prevent liquid from flowing into it. The column was then filled with liquid to a height of 6 in. above the level of the orifice. After the liquid level had been properly adjusted, the rotameter was set to give the desired gas-flow rate. At low rates of gas flow the frequency of formation of the bubbles was determined by visual inspection; at the higher rates of gas flow the frequency of formation was measured by a Stroboscope.

The data for the rate of formation of bubbles were taken at normal flow rates, or gas-flow rates above which a continuous stream of gas issues from an orifice. At gas-flow rates higher than the normal flow rates the bubble formation was not uniform and could not be determined with a stroboscope.

Experiments 232 through 243 and 561 through 575 were made under identical operational conditions. In a comparison of these data a smooth curve (frequency as a function of the gas-flow rate) was determined by the method of the least squares for each set of results. The average deviation of the experimental values with respect to the corresponding calculated values was 3 % for each set of results. The frequencies given by the smooth curve representing experiments 561 through 575 were on the average (taken over the range of flow rates employed in the two sets of

*Tabular material has been deposited as document No. 5969 with the American Documentation Institute, Photoduplication Service, *Library of Congress*, Washington 25, D. C., and may be obtained for $3.75 for photoprints or $2.00 for 35-mm. microfilm.

experiments) 4% below those given by the smooth curve for runs 232 through 243. Also the data from both sets of experiments were used to determine a single smooth curve for which an average deviation of 5% was obtained.

The room temperature was maintained at approximately 25°C. throughout the course of the investigation.

Description of Bubble Formation

Two types of bubble formation occurred. At low rates of gas flow the volume of the bubble remained relatively constant, but the frequency of formation increased as the gas-flow rate was increased. At the higher rates of gas flow the frequency of formation of the bubbles remained relatively constant, but the volume of the bubble increased as the flow rate was increased.

At low flow rates the bubbles formed singly at the orifice with a given time interval between the formation of each bubble. However as the flow rate was increased, the bubbles began to form in pairs; that is, two bubbles would appear to form simultaneously, a given time interval would elapse, and then two more bubbles would form. As the flow rate was increased further, the bubbles formed in groups of three, four, or five. Again a group would form, a given time interval would elapse, and another group would form. The time interval of course depended on the number of bubbles in the group and the rate of gas flow. This multiple bubble formation was not always reproducible. Experimental conditions that would yield groups of four might when repeated yield groups of three. In the computation of the volumes of the bubbles, however, it was assumed that they formed singly with equal time intervals between the formation of each bubble. On this basis it was found that with a given set of experimental conditions the calculated volumes of the bubbles were the same regardless of the number of bubbles in the group. Additional increases in the gas rate resulted in the formation of single bubbles at equal time intervals. This regular bubble formation continued, as the gas rate was increased, until irregular bubble formation occurred at higher flow rates, at which it was impossible to obtain quantitative data with a stroboscope.

EFFECTS OF VARIOUS DIMENSIONS OF THE APPARATUS ON THE FORMATION OF BUBBLES

The purpose of the experiments discussed in this section was to establish the approximate range over which the geometry of the apparatus could be altered without any significant deviations from the results upon which the correlations were based. Most of the geometrical quantities discussed here have been investigated with systems having zero chamber volume, although in some instances larger volumes were employed.

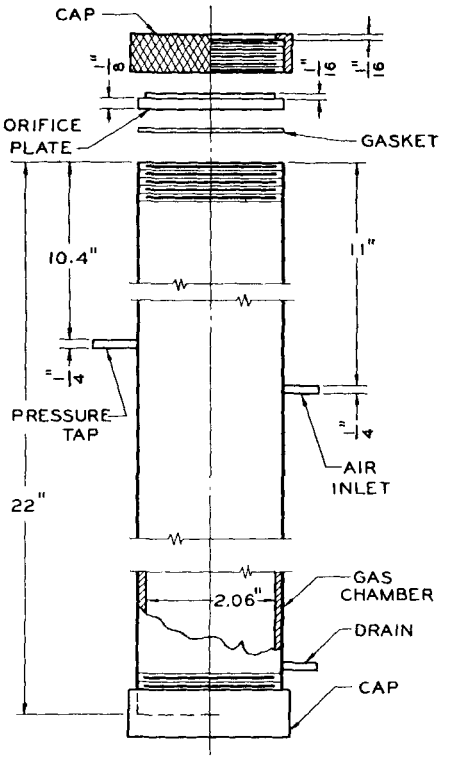

Fig. 1. Orifice holder

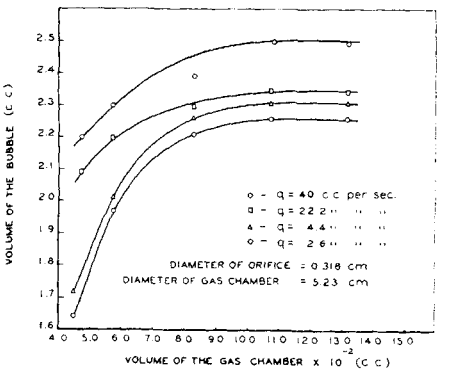

Fig. 2. Variation of the volume of the bubble with the volume of the gas chamber.

Except as noted, the experiments discussed below were performed at the following conditions: (*a*) the orifices were submerged beneath 15.2 cm. of water (*b*) the volume of the gas chamber was 1,322 cc., (*c*) the internal diameter of the gas chamber was 5.23 cm., (*d*) the thickness of the orifice plates was 0.318 cm., and (*e*) air was used in all the experiments.

The height of liquid above the orifice plate was varied from 45.7 to approximately 2.54 cm. Over the range of heights investigated the formation of bubbles appeared to be independent of the height of liquid, provided the height of liquid was greater than approximately two bubble diameters. This result is in agreement with the findings of Davidson *et al.* (*1*).

In another set of experiments the effect of the volume of the gas chamber on the formation of bubbles was investigated. In these experiments (Figure 2) the diameter of the gas chamber was held constant at 5.23 cm., and its volume was varied by partially filling it with water. For the experimental conditions stated it is evident that the formation of bubbles is independent of the chamber volume, provided that the latter is greater than about 800 cc. This result is in agreement with the concepts developed by Hughes (*4*).

As the diameter of the gas chamber is decreased, the diameter of the orifice is approached in the limit, where the formation of bubbles is said to occur at zero gas-chamber volume. In contrast, the data used in the correlations given in a subsequent section were obtained at the condition of "infinite" gas-chamber volume (or constant pressure within the gas chamber). For the experiments performed, the effect of the diameter of the gas chamber was insignificant in the formation of bubbles, provided that the ratio of the internal diameter of the gas chamber to that of the orifice was equal to or greater than 4.5. Actually the lower limit lies between 1.0 and 4.5, since the results of experiments performed at the limit stated, $D_c = 1.43$ cm., $D_0 = 0.318$ cm., were in agreement with those obtained with an orifice diameter of 0.318 cm. and gas chamber diameters of 2.69, 5.23, and 10.3 cm.

The effect of the thickness of the orifice plate on the formation of bubbles was also investigated. It should be pointed out that as the thickness of the orifice plate is increased indefinitely, the condition of zero chamber volume is approached in the limit. Capillary tubes were used as orifice plates in those experiments where plate thickness greater than 0.318 cm. were employed. These tubes were attached to a gas chamber having a volume of 1,322 cc. For the flow rates (corresponding to the region of relatively constant frequency) employed, the effect of the thickness of the orifice plate on the formation of bubbles became significant at thicknesses equal to or greater than 100 orifices diameters, in agreement with the results of Hughes (*4*). Orifices having diameters of 0.318 and approximately 0.635 cm. were used in this set of experiments. If a lower limit of the ratio of the plate thickness to the orifice diameter exists, it appears to lie below 0.5 (obtained with an orifice diameter of 0.318 cm. and a plate thickness of 0.159 cm.). The results corresponding to the latter ratio were in agreement with those obtained when both a plate thickness and an orifice diameter of 0.318 cm. were employed.

DEVELOPMENT OF EQUATIONS

The analysis of the formation of bubbles at submerged orifices is concerned with the forces acting on the surface of the bubble, as would be seen

by a stationary observer located at any point exterior to the bubble. The various forces acting were related through the application of Newton's second law of motion.

In the following analysis of this process the actual bubble was replaced by one of equal mass, which moved with the average vertical-component velocity and had the same forces acting on it as those which acted on the actual bubble.

First the center of a spherical bubble is considered fixed and the bubble allowed to expand equally in all directions. Then

$$\frac{dV}{dt} = q \tag{1}$$

Furthermore

$$\frac{dV}{dt} = \frac{dV}{dD}\frac{dD}{dt} = \pi D^2 \frac{dr}{dt} \tag{2}$$

For convenience

$$v_n = \frac{dr}{dt} = \frac{q}{\pi D^2} \tag{3}$$

The growth of a spherical bubble at a submerged orifice may be represented as shown in Figure 4. To obtain the velocity of a point on the surface of a bubble at any instant during its formation, it is convenient to think of a given growth process of a bubble at an orifice as being composed of two steps: first, that the center of a given bubble is fixed and that the bubble experiences an expansion in unit time such that its radius is increased by an amount v_n, and, second, that each point on the surface of the bubble so formed is displaced vertically by an amount v_n in unit time. The vector representation of this two-step growth process is shown in Figure 5. The subscripts 1 and 2 of the vectors $\mathbf{v}_{n_1}$ and $\mathbf{v}_{n_2}$ denote the steps just mentioned. The velocity $\mathbf{v}_R$ of any given point on the surface of the bubble is of course the vector sum of $\mathbf{v}_{n_1}$ and $\mathbf{v}_{n_2}$, as indicated in Figure 5. Thus

$$\mathbf{v}_R = \mathbf{v}_{n_1} + \mathbf{v}_{n_2} \tag{4}$$

The magnitude of the vertical component of $\mathbf{v}_R$ is given by the dot product $\mathbf{v}_R \cdot \mathbf{j}$, as

$$\mathbf{v}_R \cdot \mathbf{j} = \mathbf{v}_{n_1} \cdot \mathbf{j} + \mathbf{v}_{n_2} \cdot \mathbf{j} = v_y \tag{5}$$

By definition of the dot product

$$v_y = (v_{n_1})(1) \cos\left(\frac{\pi}{2} - \alpha\right) + (v_{n_2})(1) \cos(0) \tag{6}$$

and

$$v_y = v_{n_1} \cos\left(\frac{\pi}{2} - \alpha\right) + v_{n_2} \tag{7}$$

Since

$$\sin\alpha = \cos\left(\frac{\pi}{2} - \alpha\right) \tag{8}$$

and since $v_{n_1} = v_{n_2} = v_n$, Equation (7) may be written as

$$v_y = v_n(1 + \sin\alpha) \tag{9}$$

Examination of Equation (9) shows that v_y is symmetrical about the vertical axis of the bubble. Thus the average of v_y over a circle containing the vertical axis as a diameter is equal to the average of v_y over the entire surface. Then

$$v(2\pi r) = \int_0^{2\pi} v_y r \, d\alpha \tag{10}$$

When the expression for v_y as a function of α [Equation (9)] is substituted in the preceding expression, one obtains upon integration

$$v = v_n \tag{11}$$

where v_n is of course defined by Equation (3).

The formation of a bubble at a submerged orifice is a variable-mass type of problem. Pars (*8*) has shown that when to a body of mass which is moving with the instantaneous velocity v (relative to a fixed observer), mass traveling with the velocity v_0 (relative to a fixed observer) is added at the rate dm/dt, one must include the force v_0 (dm/dt) in the application of Newton's second law of motion. In addition to this force, a bubble is also acted upon by the following forces during its formation: the net bouyancy force $gV\Delta\rho$ and the excess pressure force $(\pi D_0^2/4)$ $(p_i - p)$, the surface tension force $\pi D_0\sigma$, the drag force, and the force required to overcome the inertia of the fluid surrounding the bubble. For a bubble moving with the instantaneous velocity, the latter force is given by m' (dv/dt). Thus when the actual bubble is replaced by one moving with the instantaneous velocity and with the same set of forces acting on its external surface and when the vertical direction is taken as positive, one obtains by application of Newton's second law

$$v_0 \frac{dm}{dt} + gV\Delta\rho + \frac{\pi D_0^2}{4}(p_i - p) - \pi D_0\sigma - F - m'\frac{dv}{dt} = \frac{d(mv)}{dt} \tag{12}$$

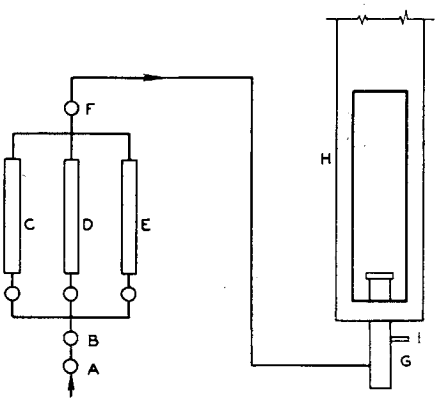

Fig. 3. Flow diagram of equipment: A—air inlet; B—pressure regulators; C, D, E—rotameters; F—¼-in. needle valve; G—orifice holder; H—column; I—connection for open-end manometer.

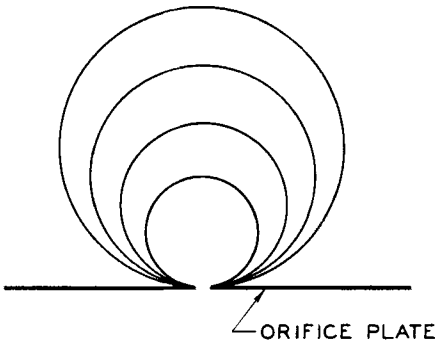

Fig. 4. Formation of a spherical bubble at a submerged orifice.

The pressure in the liquid at the level of the orifice is slightly less than the pressure of the gas at the top edge of the orifice because of the effect of surface tension. When the net buoyancy force is taken to be $gV\Delta\rho$, it is implied that the pressure, p, instead of the actual pressure, p_i, acts over the area of the bubble immediately above the orifice. In accordance with the treatment of Hughes *et al.* (*4*), the excess pressure force was included to account for the error in the expression for the net bouyancy force. The fact that a pressure slightly greater than p_i is required for the gas to flow from the top of the orifice to the various parts of an expanding bubble is neglected in the present treatment. Since the diameter of the orifice was always small as compared with that of the bubble, the excessive pressure force was relatively small. Because of the large chamber volumes employed, the pressure within the chamber was approximately constant and the well-known relationship

$$p_i - p = \frac{4\sigma}{D} \tag{13}$$

was employed for the evaluation of the excessive pressure force at the instant just prior to the release of the bubble from the orifice. Prandtl (*9*) has given an informative derivation of this relationship. It should also be pointed out that in the calculation of q the pressure within the gas chamber was employed, because in all experiments the pressure drops across the orifice were less than 1 in. of water.

Other terms in Equation (12) may be evaluated also at the instant just prior to the release of the bubble. When the first member of the left-hand side of

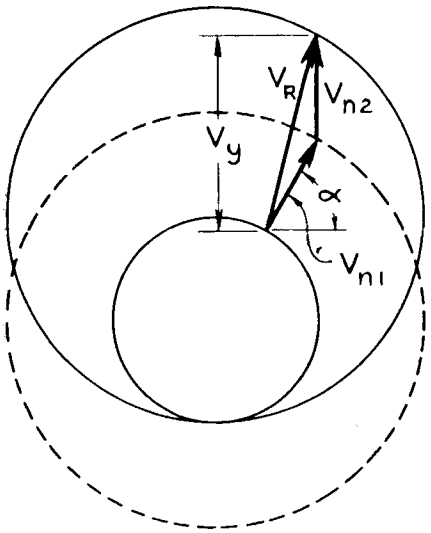

Fig. 5. Velocity of a point on the surface of a bubble during formation.

Equation (12) is transposed to the right-hand side, the latter becomes

$$\frac{d(mv)}{dt} - v_0\frac{dm}{dt} = m\left(\frac{dv}{dD}\right)\left(\frac{dD}{dt}\right) + (v - v_0)\frac{dm}{dt} \tag{14}$$

Substitution of $2v$ for dD/dt and $q\rho_g$ for dm/dt in Equation (14) yields

$$\frac{d(mv)}{dt} - v_0\frac{dm}{dt} = (2mv)\left(\frac{dv}{dD}\right) + (v - v_0)(q\rho_g) \tag{15}$$

Since $v = q/\pi D^2$, $dv/dD = (-2q)/(\pi D^3)$, $v_0 = (4q)/(\pi D_0^2)$, and $m = V\rho_g$, it is readily shown that the above expression reduces to

$$\frac{d(mv)}{dt} - v_0\frac{dm}{dt} = -\frac{4q^2\rho_g}{\pi D_0^2}\cdot\left[1 - \frac{1}{12}\left(\frac{D_0}{D}\right)^2\right] \tag{16}$$

The total drag force was expressed in terms of the drag coefficient as

$$F = \frac{c_D\rho_L v^2 A_f}{2} \tag{17}$$

When the the assumption of spherical bubbles is made, the representative area may be replaced by $\pi D^2/4$. Since $v = q/\pi D^2$, the drag force is readily stated in terms of the Froude number, the drag coefficient, and the volume of the bubble; that is,

$$F = \frac{c_D\rho_L v^2 A_f}{2} = \left(\frac{c_D\rho_L}{2}\right)\left(\frac{q^2}{\pi^2 D^4}\right)\left(\frac{\pi D^2}{4}\right) \tag{18}$$

$$F = \frac{3g\rho_L c_D N_{Fr} V}{4}$$

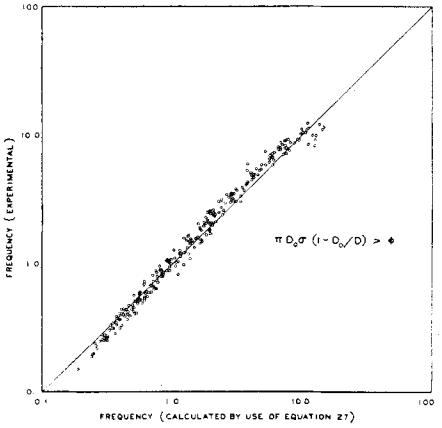

Fig. 6. Comparison of experimental and calculated values of the frequency of bubble formation.

where the Froude number is defined by

$$N_{Fr} = \frac{v^2}{Dg} = \frac{q^2}{\pi^2 D^5 g} \tag{19}$$

In the consideration of the last term on the left-hand side of Equation (12) Streeter (*10*) has shown that in the case of irrotational motion m' equals one half of the mass of the displaced fluid. Although in the present case the flow was not irrotational, m' was taken proportional to the mass of the displaced fluid. Thus

$$m'\frac{dv}{dt} = \rho_L V\chi\left(\frac{dv}{dt}\right) = \rho_L V\chi\left(\frac{dv}{dD}\right)\left(\frac{dD}{dt}\right) \tag{20}$$

When the derivatives appearing in the right-hand member are evaluated as outlined previously in the treatment of Equation (14), one obtains

$$m'\frac{dv}{dt} = \rho_L V\chi\left(\frac{-2q}{\pi D^3}\right)\left(\frac{2q}{\pi D^2}\right) = -4\rho_L g\chi N_{Fr} V \tag{21}$$

For irrotational motion the quantity χ is of course equal to $\frac{1}{2}$, but since it was not irrotational, the quantity χ and the drag coefficient were correlated as a power function of the appropriate dimensionless groups.

When the results given by Equations (13), (16), (18), (21) are substituted in Equation (12), it reduces to

$$V\Delta\rho_g(1 - \psi) = \pi D_0\sigma\left(1 - \frac{D_0}{D}\right) - \phi \tag{22}$$

The symbols ψ and ϕ, introduced for convenience, have the following definitions:

$$\psi = \left(\frac{3\rho_L}{4\Delta\rho}\right)(N_{Fr})\left[c_D - \frac{16}{3}\chi\right] \tag{23}$$

$$\phi = \frac{4q^2\rho_g}{\pi D_0^2}\left[1 - \left(\frac{1}{12}\right)\left(\frac{D_0}{D}\right)^2\right] \tag{24}$$

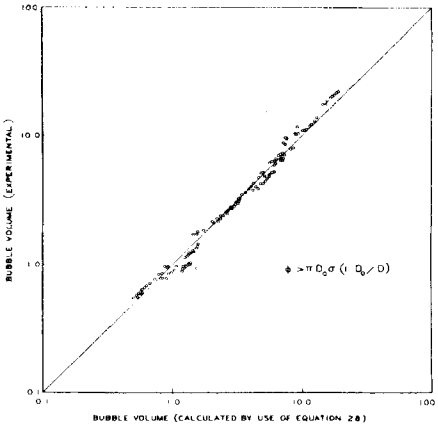

Fig. 7. Comparison of experimental and calculated values of the bubble volume.

The use of Equation (22) in the correlation of the experimental results follows.

CORRELATIONS

The variables contained in Equation (22) were evaluated at the instant just prior to the release of the bubble from the orifice. Since the drag coefficient is a function of the Reynolds number, Equation (23) demonstrates that ψ is a function of both the Froude and Reynolds numbers. Because of the relative magnitudes of the terms constituting Equation (22), the direct solution for and correlation of $(c_D - 16/3\ \chi)$ proved impractical; instead the positive difference of $(1 - \psi)$ was correlated.

Since the diameter of the bubble was always considerably greater than the diameter of the orifice, the expression for ϕ reduces to $(4q^2\rho_g)/(\pi D_0^2)$, which is the time rate of change of momentum of the gas added to the bubble at the instant just prior to its release from the orifice. In effecting a correlation, the data were divided into two groups. The first group consisted of the runs for which $\pi D_0\sigma(1 - D_0/D) > \phi$; that is, the net-surface tension force was greater than the time rate of change of the momentum of the gas added to the bubble. In the actual classification of the runs the complete expression for ϕ [given by Equation (24)] was employed.

The experimental value for the positive difference of $(1 - \psi)$ was obtained indirectly by the experimental determination of the remaining terms of Equation (22). For each set of data the absolute value of $(1 - \psi)$ was correlated as a power function of the Froude number, the Reynolds number, and the ratio D_0/D as

$$|(1 - \psi)| = K(N_{Re})^a(N_{Fr})^b\left(\frac{D_0}{D}\right)^c \tag{25}$$

where

$$N_{Re} = \frac{Dv\rho_L}{\mu_L} = \frac{q\rho_L}{\pi D\mu_L} = \frac{q^{2/3}f^{1/3}\rho_L}{\pi^{2/3}6^{1/3}\mu_L} \tag{26}$$

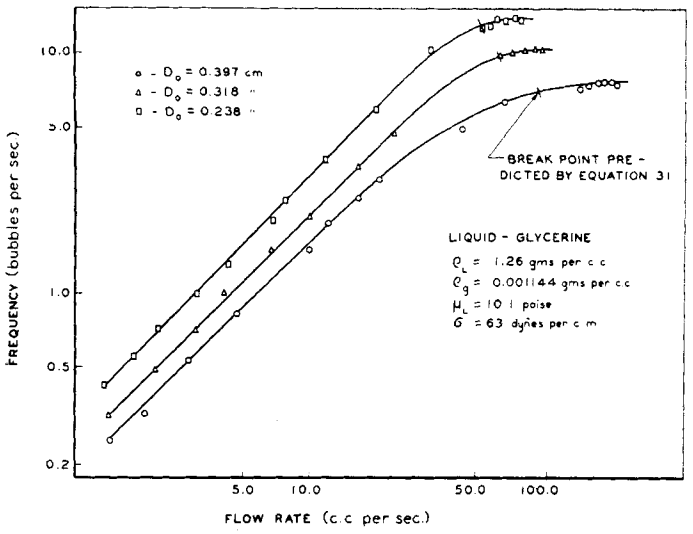

Fig. 8. Prediction of the division of the two ranges of bubble formation.

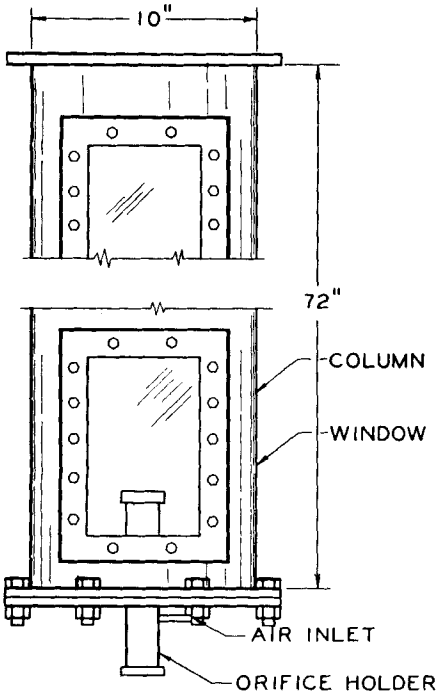

Fig. 9. Experimental column.

For those runs for which $\pi D_0\sigma\ (1 - D_0/D) > \phi$, the volume of the bubble varied little with the gas-flow rate, but the frequency of bubble formation changed appreciably with the gas-flow rate. In the upper range of flow rates [for which $\phi > \pi D_0\sigma\ (1 - D_0/D)$] the situation just described was reversed. In view of these physical considerations the frequency of bubble formation was selected as the dependent variable for those experiments where $\pi D_0\sigma\ (1 - D_0/D) > \phi$. For the range of flow rates in which $\phi > \pi D_0\sigma\ (1 - D_0/D)$, the volume of the bubble was taken as the dependent variable.

When Equation (22) is solved for V, one obtains V as a function of V, since $(1 - \psi)$ is also a function of V. Similarly, since $V = q/f$, Equation (22) may be solved for the frequency as a function of the frequency. For those data in the range $\pi D_0\sigma\ (1 - D_0/D) > \phi$, the best correlation for the calculation of the frequencies (or bubble volumes) was obtained by the use of the expression obtained by solving Equations (22) and (25) for f as a function of the other variables. Actually the diameter of the bubble was left in the expression for ϕ, since the latter was relatively insensitive to the bubble diameter. The following correlation was obtained. For $\pi D_0\sigma\ (1 - D_0/D) > \phi$

$$f = \frac{7.56 \times 10^{-3}}{\bar{N}_{Re}^{\ 3}} (\bar{N}_{Fr}\bar{N}_{Re}^{-5})^{-0.172} \cdot (Nq\bar{N}_{Re}^{\ 3})^{0.525} \left[\frac{D_0\bar{N}_{Re}^{\ -1}}{\left(\frac{6q}{\pi}\right)^{1/3}}\right]^{-0.697} \quad (27)$$

where

$$\bar{N}_{Fr} = N_{Fr}f^{-5/3} = \frac{q^{1/3}}{g\pi^{1/3}\ 6^{5/3}}$$

= modified Froude number

$$\bar{N}_{Re} = N_{Re}f^{-1/3} = \frac{q^{2/3}\rho_L}{\pi^{2/3}6^{1/3}\mu_L}$$

= modified Reynolds number

$$N = \left|\frac{\pi}{6}\left(\frac{\Delta\rho g}{\pi\ D_0\sigma(1 - D_0/D) - \phi}\right)\right|$$

Those data falling in the variable volume range were correlated in a similar manner by solving Equations (22) and (25) for the volume of the bubble as a function of the other variables. Again the diameter of the bubble was left in the expression for ϕ because the latter was relatively insensitive to this diameter. The correlation for these data follows. For $\phi > \pi D_0\sigma\ (1 - D_0/D)$

$$V = \frac{23.4}{N} (N_{Fr}'N^{5/3})^{0.463} \cdot (N_{Re}'N^{1/3})^{-0.0764}(D_0N^{1/3})^{0.712} \quad (28)$$

where

$$N_{Fr}' = N_{Fr}\ D^5$$

$$N_{Re}' = N_{Re}\ D$$

Equations (27) and (28) apply for the case of infinite chamber volume. The constants and exponents in Equations (27) and (28) were determined by the method of the least squares through the use of a digital computer. The average percentage deviations of the calculated values of f and V [as given by Equations (27) and (28)] from the experimental values were 16 and 10 repectively. The corresponding correlation coefficients were 0.998 and 0.988. Graphs of the experimental values of f and V vs. the values calculated by the use of Equations (27) and (28) are shown in Figures 6 and 7. The significance of each of the groups in these equations was shown by the determination of the correlation coefficient and the average percentage deviation when each of the terms shown in the equation was omitted and the others were retained. When each of the groups containing the modified Froude number, the term (Nq), and the diameter of the orifice was omitted from Equation (27) and the others were retained, the correlation coefficients were 0.994, 0.994, and 0.997, respectively, and the corresponding average percentage deviations were 3×10^8, 44, and 1.4×10^9. Similarly, omission of the groups containing the modified Froude number, the modified Reynolds number, the diameter of the orifice, and the retention of all the other groups in Equation (28) gave the following correlation coefficients: 0.976, 0.965, and 0.984 respectively. The corresponding average percentage deviations were 69, 16, and 11. Thus all the terms shown in Equation (27) are required in order to represent adequately the experimental results. In the process of correlating the data, a surface-tension number [defined in the same manner as the one used by Hughes *et al.* (4)] was used together with those groups shown in Equations (27) and (28), and the average percentage deviations were only about 1% better than those given by Equations (27) and (28).

It is to be observed that little accuracy was lost when the term containing the diameter of the orifice was omitted in the correlation of the data for the upper region of the flow rates. In view of this the correlation is included.

For $\phi > \pi D_0\sigma\ (1 - D_0/D)$

$$V = \frac{5.94}{N} (N_{Fr}'N^{5/3})^{0.745} \cdot (N_{Re}'N^{1/3})^{-0.0637} \quad (29)$$

It should also be mentioned that when stated in terms of the diameter of the bubble, the average percentage deviations of the experimental values of D from the values calculated by the use of Equations (27) and (28) were 5.0 and 3.0 respectively.

Some experiments were performed in which a silicone additive was used to alter the surface tension of the liquid. Those results were not employed in the determination of the constants for Equations (27) and (28) because in some instances (7) such liquid mixtures do not appear to exhibit the characteristics of pure liquids having the same apparent physical properties. The average percentage deviations of the experimental value of the dependent variable from the value calculated by the use of Equations (27) and (28) were 25 and 30 % respectively. The relatively poor agreement lends further support to the characteristics just discussed.

DISCUSSION

A comparison of the volumes of the bubbles obtained in the present work with those of other workers who employed essentially zero chamber volumes shows that at similar operating conditions the volumes of the bubbles obtained by the use of the system described herein (operation was at constant pressure within the gas chamber, or infinite gas-chamber volume) were always larger. The equations stated by Hughes *et al.* (4) and given the numbers 19, 20, 23 and 24 did not correlate the data obtained by the authors nearly so well as did Equations (27) and (28), perhaps because of the large gas-chamber volumes employed in the present work.

The theoretical treatment of the formation of bubbles led to a description of the two regions of bubble formation as well as a physical explanation for the division of the two regions. As discussed previously, at low gas-flow rates the surface-tension force was greater than than the time rate of change of the momentum of the gas entering the bubble, while at the higher rates of gas flow the order of magnitude of the two forces was reversed. Furthermore, according to the theory developed for the case of infinite chamber volume, the division of the two regions occurred when there was an equality between the two forces, namely

$$\pi D_0\sigma(1 - D_0/D) \cong \frac{4q^2\rho_g}{\pi D_0^2} \qquad (30)$$

or

$$q = \frac{\pi}{2}\sqrt{\frac{D_0^3\sigma(1 - D_0/D)}{\rho_g}} \qquad (31)$$

In Figure 8 the experimental results as well as the predicted division of the two ranges are shown. Although there is no sharp division between the lower range of relatively constant bubble volume and variable frequency of formation and the upper range of relatively constant frequency and variable bubble volume, the division predicted by Equation (31) appears adequate.

ACKNOWLEDGMENT

This work was supported by the E. I. du Pont de Nemours and Company, Humble Oil and Refining Company, and The Texas Engineering Experiment Station. This aid is gratefully acknowledged. Helpful suggestions offered by D. M. Vestal of the Experiment Station are also appreciated.

NOTATION

A_f = representative area of the bubble, $\pi D^2/4$ for spheres; L^2

c_D = drag coefficient, dimensionless

D = diameter of the bubble (assumed to have a spherical shape), L

D_0 = diameter of the orifice, L

F = drag force, the sum of the vertical components of the viscous and form drag forces, ML/T^2

f = frequency of bubble formation

g = acceleration of gravity, L/T^2

g_c = conversion factor, ML/T^2F

$\mathbf{j}$ = unit vector in the vertical direction, dimensionless

L = thickness of the orifice plate in the direction of flow, L

m = mass of the bubble at any time, t; M

m' = mass term for the displaced fluid, M

N = a term defined below Equation (27), L^{-3}

N_{Fr} = Froude number defined by Equation (19), dimensionless

N_{Re} = Reynolds number defined by Equation (26), dimensionless

p = pressure in the liquid at the level of the top of the orifice, M/LT^2

p_i = static pressure of the gas stream at the level of the exit side of the orifice plate, M/LT^2

q = volumetric rate of gas flow evaluated at the conditions at the top of the orifice, (because of the small pressure drops involved the pressure was taken equal to that of the gas chamber in the calculation of q), L^3/T

t = time, T

v = average of the vertical component of velocity over the surface of the bubble, L/T

$\mathbf{v}_{n_1}, \mathbf{v}_{n_2}$ = vectors having the magnitude v_n given by Equation (4) and directions indicated in Figure 5, L/T

$\mathbf{v}_R$ = velocity vector of any point on the surface of a bubble during its formation at a submerged orifice, L/T

v_y = magnitude of the vertical component of the velocity v_R, L/T

v_0 = velocity at which the gas flows through the orifice, L/T

V = volume of the bubble at the instant just prior to its release from the orifice, L^3

Greek Letters

α = angle used in the vector diagram (Figure 5), radians

$\Delta\rho$ = density of the liquid minus the density of the gas, M/L^3

μ_L = viscosity of the liquid, M/LT

π = 3.1416

ρ_g = density of the gas evaluated at the temperature and pressure of the gas chamber, M/L^3

ρ_L = density of the liquid in which the orifice plate was submerged, M/L^3

σ = interfacial tension of the liquid with respect to air, M/T^2

ϕ = a variable which was approximately equal to the time rate of change of the momentum of the gas entering the bubble, defined by Equation (24), ML/T^2

χ = a function defined by Equation (20), dimensionless

ψ = a function defined by Equation (23), dimensionless

Mathematical Symbols

$|x|$ = absolute value of x

LITERATURE CITED

1. Davidson, Leon, and Edwin H. Amick, Jr., *A.I.Ch.E. Journal*, **2**, No. 3, 337 (1956).
2. Eversole, W. G., G. H. Wagner, and Eunice Stackhouse, *Ind. Eng. Chem.*, **33**, 1459 (1941).
3. Hayes, William B., III, dissertation, Agricultural and Mechanical College of Texas, College Station, Texas (May, 1958).
4. Hughes, R. R., A. E. Handlos, H. D. Evans, and R. L. Maycock, *Chem. Engr. Progr.*, **51**, No. 12, 557 (1955).
5. Leibson, Irving, E. G. Holcomb, A. G. Cacoso, and J. J. Jacmic, *A.I.Ch.E. Journal*, **2**, No. 3, 296 (1956).
6. *Ibid.*, **2**, No. 3, 300 (1956).
7. Pattle, R. E., *Trans. Inst. Chem. Engrs. (London)*, **28**, 32 (1950).
8. Pars, L. A., "Introduction to Dynamics," pp. 162 to 165, Cambridge University Press, Cambridge, England (1953).
9. Prandtl, Ludwig, "Essentials of Fluid Dynamics, Authorized translation, pp. 26 to 30, Hafner Publishing Company, New York (1952).
10. Streeter, V. L., "Fluid Dynamics," pp. 64 to 67, McGraw-Hill, New York (1948).

Manuscript received July 7, 1958; revision received December 29, 1958; paper accepted December 30, 1958.